Scripta Materialia 159 (2019) 72–75

Contents lists available at ScienceDirect

Scripta Materialia

journal homepage: www.elsevier.com/locate/scriptamat

Regular article

Graphite assisted flash sintering of Sm_2O_3 doped CeO_2 ceramics at the onset temperature of 25 °C

Lili Guan, Jian Li, Xiwen Song *, Jinxiao Bao, Tao Jiang

Inner Mongolia Key Laboratory of Advanced Ceramics and Device, School of Materials and Metallurgy, Inner Mongolia University of Science and Technology, Baotou 014010, China

ARTICLE INFO

Article history:
Received 1 August 2018
Received in revised form 10 September 2018
Accepted 10 September 2018
Available online 15 September 2018

Keywords:
Graphite assisted flash sintering
Direct current electric field
Sm_2O_3 doped CeO_2 ceramics
Room temperature

ABSTRACT

Flash sintering of Sm_2O_3 doped CeO_2 ceramics can be triggered at 25 °C due to the presence of graphite. The current density rise non-linearly to a set limit value in the voltage control stage under an initial electric field of 30 V cm^{-1}. The calculated conductivity activation energy in this stage is 0.30 eV, which is closely in relation to the electronic conduction of graphite. As graphite is beginning to oxidize, the conductivity of the sample rapidly decreases. While graphite has been completely oxidized, the specimen temperature provides adequate support for the persistence of flash sintering process.

The flash sintering technique can realize the densification of materials at a much lower temperature by applying a direct current electric field than conventional sintering, thus it has been attracted significant attention in recent years. Cologna and Raj firstly reported that 3 mol% yttrium-stabilized zirconia (3YSZ) can be sintered in a few seconds at 850 °C to full density at a field of 120 V cm^{-1} [1]. After that, this technique has been applied to sintering of a wide range of ceramics including ionic conductors, electronic conductors, semiconductors and insulators [2–8]. Yadav and Raj summarized the flash sintering process of several oxides, such as Co_2MnO_4, YSZ, $BaTiO_3$, ZnO, TiO_2, MgO doped Al_2O_3, etc. [9]. The onset temperature of flash sintering ranges from 300 °C to 1300 °C, when the electric field varies from 7.5 V cm^{-1} to 1000 V cm^{-1}, which suggests that the flash sintering process of an oxide requires a certain starting temperature. Moreover, lowering the onset temperature of the flash sintering for a certain oxide should increase the direct current electric field. Down and Sglavo showed that the onset temperature of 8YSZ could be decreased to 390 °C under a high electric field of 2250 V cm^{-1}, however only moderate densification (i.e., ~8.5% linear shrinkage) was achieved, meaning the ceramics is not fully densified [10]. Therefore, it is necessary to develop the flash sintering technique to achieve high-density ceramics at relatively low starting temperature.

Recently, Luo et al. successively demonstrated that dry and wet reduced atmosphere (Ar + 5 mol% H_2) can significantly lower the onset temperature of ZnO to <120 °C and 25 °C, respectively, which should be ascribed to the hydrogen interstitials increasing the specimen conductivity at lower temperature [11,12]. This provides us an approach to decrease the onset flash sintering temperature by improving the electrical conductivity of the green bodies. The introduction of graphite into the green body of ceramics would trigger a thermal runaway at a lower temperature, leading to the occurrence of flash sintering. The aim of the present work is to investigate the feasibility for graphite assisted flash sintering (GAFS) of Sm_2O_3 doped CeO_2 (SDC) ceramics at room temperature.

10 mol% Sm_2O_3 doped CeO_2 powders were synthesized by a citrate-nitrate combustion method. The mixture of SDC and graphite powders (5% in mass percent, Aladdin, 99.95% metals basis) was acquired by milling them in a planetary ball mill using zirconia pot and balls, then uniaxially pressed under 300 MPa into green pellets. The samples had a length of 5 mm and a rectangular cross section of 3 mm × 1 mm. Silver paste was manually painted on both sides of compacted specimens and fired at 200 °C for 30 min to make the Ag electrodes. Then it was loaded into a quartz tube to connect with Ag wires for applying electric field/current. The power was supplied and monitored by a digital multimeter (Series 2420, Keithley). It was automatically switched to a current control mode once the flash current reached the preset maximum value. In order to avoid sudden power surge forming a hot spot, even damage to the internal structure of the specimens, a stepwise increase in the current density by 2.5 A cm^{-2} was adopted. The sintering process under the maximum current density of 20 A cm^{-2} lasted for 10 min. The electrical conductivity of the samples was calculated using the 4-terminal method by *IL/VS*. Where *V* is the voltage in the circuit, *I* is the current value, *L* and *S* are the length and sectional area of the specimen, respectively, ignoring the dimensional change of samples during flash sintering. The microstructures were characterized by a field emission scanning electron microscope (FESEM, Philips XL30). The grain sizes of specimens were measured using the linear intercept method.

* Corresponding author.
E-mail address: songxiwen@imust.cn (X. Song).

https://doi.org/10.1016/j.scriptamat.2018.09.014
1359-6462/

In our previous study, a flash sintering process of SDC ceramics under a direct current electric field was studied [13]. The results show that there is an abrupt increase in the current when the electric field is above 60 V cm^{-1}, the corresponding temperature is known as the onset of the flash event. It had been reported that the application of an electric field as high as 120 V cm^{-1} permitted the full densification within 10 min of SDC at temperature of 578 °C. Fig. 1 shows the comparison of three sintering methods. The electric current as a function of the environment temperature for the conventional sintering (CS, under an electric field of 0 V cm^{-1}), flash sintering (FS, under an electric field of 120 V cm^{-1}), and graphite assisted flash sintering (GAFS, under an electric field of 30 V cm^{-1}) is given in Fig. 1(a). Similiar to the FS process, the electric current of GAFS process also has an abrupt increase. Whereas, GAFS process exhibits an abrupt current increase under an electric field of 30 V cm^{-1}, significantly different from the FS process which shows an abrupt current increase under an electric field of 120 V cm^{-1}. This diviation should be ascribed to the mixed electronic and ionic conductivity of the SDC and graphite composite. In particular, the onset temperature of GAFS is 25 °C, which is significantly lower than the onset temperature of FS (578 °C). This indicates the possibility for the flash effect of ceramics at room temperature.

To identify the microstructures of the ceramics sintered by GAFS technique, the micrographs of the CS, FS and GAFS samples were characterized by a field emission scanning electron microscope, as shown in Fig. 1(b) (CS at 1450 °C for 120 min with a heating rate of 5 °C min^{-1}, FS at 578 °C for 10 min and GAFS at 25 °C for 10 min, respectively). The experimental parameter and average grain size determined by the linear intercept method were listed in Table 1. As can be seen, all the sintered samples are fully dense, and samples of FS and GAFS display the fine grained structure. The average grain size of GAFS samples is 0.54 μm, and which is 0.36 μm for FS samples, all much less than that of the CS method (1.21 μm). This clearly indicates that the dense and fine grained structure can be obtained by the FS and GAFS methods, which inhibit the rapid grain growth related to the high sintering temperature and lengthy holding time [14]. In addition, graphite assisted flash sintered sample does not exist residual graphite term.

Fig. 2(a) displays the variations of the current density and electrical conductivity with time during the GAFS process. In conventional flash sintering, the current rises non-linearly to a set limit value, accompanied by a power spike [15]. This sudden larger power spike may lead to hot spot event, even destroy the structure of samples [16]. One way that the current density increasing stepwise by 2.5 A cm^{-2} was proposed [13]. In addition, according to the current variation, the conventional flash sintering is usually divided into three stages: incubation stage (I), flash sintering stage (II) and constant current stage (III) [17]. However, the process of graphite assisted flash sintering reveals different behaviour. That is a current drop at some point in a constant current mode (called it stage IV), which should be related to the oxidation of graphite. The electrical conductivity sharply increases to the peak value, and then decreases rapidly, which should be ascribed to the existence and oxidation of graphite. Subsequently it step-wisely increases towards a steady state, similiar to the controllable flash sintering process [13]. The conduction of the sample caused by graphite is substantially responsible to trigger a thermal runaway in flash sintering at room temperature [11].

To investigate the essence of decline in current in stage IV, comprehensive thermal analysis of the sample in air was performed. TG and DSC curves of SDC-5 wt% graphite composite green compact between room temperature and 1200 °C are shown in Fig. 2(b). It can be seen that the mass of the sample almost no changes at 25–559 °C. In the temperature range of 560–800 °C, the sample shows a total mass loss of 5%, indicating that graphite is completely oxidized, i.e., the electrical conductivity of the sample is sharply decreased at this moment. The decrease in conductivity results in the variation of the current. After graphite completely burnout, the current returns to the preset limit value. The actual temperature of the sample in this stage reaches the onset temperature of flash sintering for SDC. In addition, the heat released by oxidation of graphite provides an auxiliary energy of the SDC densification.

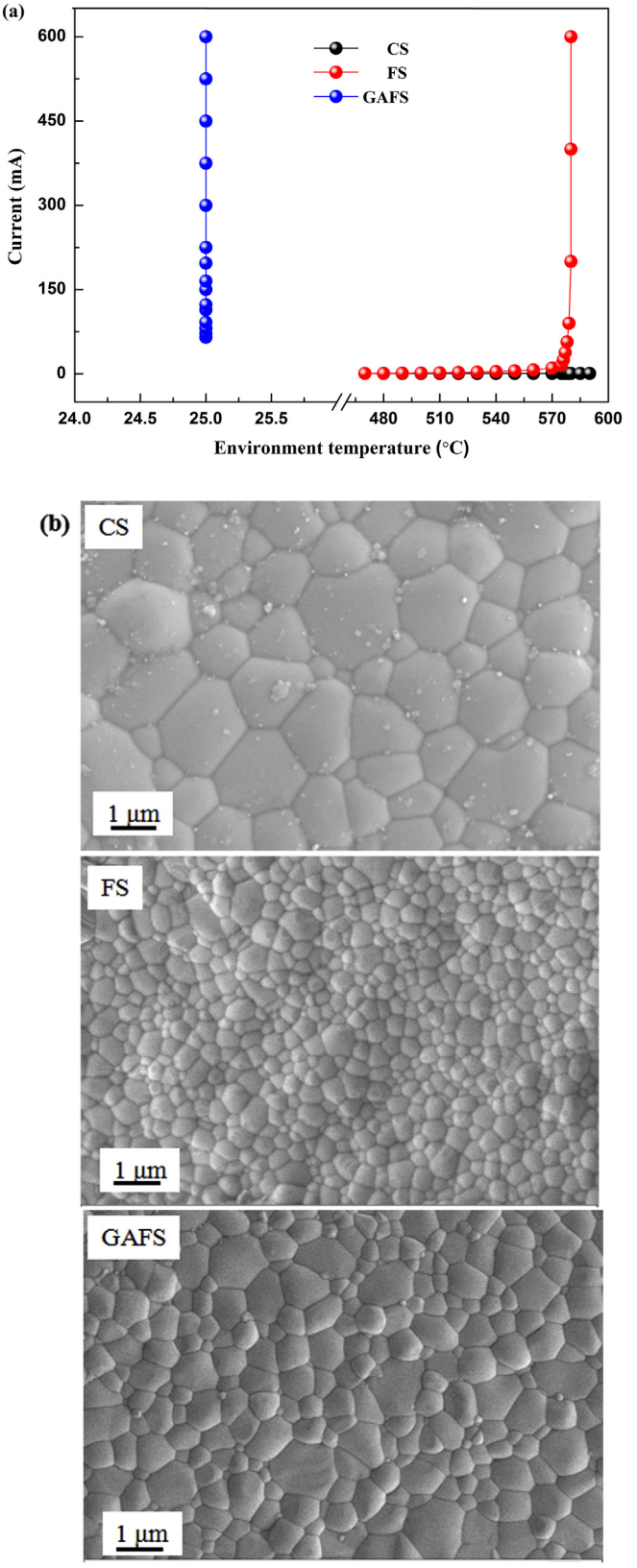

Fig. 1. Comparison of three sintering methods (a) electric current as a function of environment temperature and (b) SEM micrographs of the ceramics.

Table 1
Listing of experimental parameter, average grain size and estimated specimen temperature.

Environment temperature (T_e, °C)	Estimated specimen temperature (T_{es}, °C)	Average grain size (μm)	Initial electric field (V cm^{-1})	Current density (A cm^{-2})	Holding time (min)
CS-1450 °C [13]	1450	1.21	0	0	120
FS-578 °C [13]	1514	0.36	120	20	10
GAFS-25 °C	1285	0.54	30	20	10

Estimating the specimen temperature is of vital importance to determine the main triggering mechanisms during flash sintering process, as well to explain the variation in the material electrical conductivity [18]. The estimated temperature can be obtained by assuming that the specimen radiates like a black body with an emissivity, based upon the Stefan-Boltzmann law [6,19,20]. The assumption that radiation losses are far greater than convective heat loss to the environment. According to the black body radiation model, the estimated temperature is given by:

$$T_{es} = \left(T_e^4 + \frac{W}{\varepsilon\sigma_r A}\right)^{\frac{1}{4}}$$

where T_{es} is the estimated specimen temperature, T_e is the environmental temperature of 25 °C, W is the power dissipation (ignore the dissipated power due to the contacts), A is the total surface area of the green compact ($A = 4.6 \times 10^{-5}$ m^2 in this experiment), and σ_r is the black body radiation constant (5.67×10^{-8} W m^{-2} K^{-4} [6]), ε is the emissivity which is assumed to lie in the range of 0.8–1.0 (for most oxides this value is 0.9). The calculation process is divided into two stages according to whether the graphite is completely oxidized. The emissivity values are 0.91 and 0.9, respectively. The calculated temperatures by the power dissipation are shown in Fig. 3.

The change in power dissipation is also observed. As the time increases from 0 to 50s, the increase in the power density varies from the slow state to exponential growth, this is corresponding to stage I and II. In initial stages, the power dissipation improves to the limited maximum value, then sharply declines to a steady state, as the power supply switches from constant voltage to current constant control. The power dissipation in the stage IV is about 225, 197 and 165 mW mm^{-3}, corresponding estimated temperatures are 821 °C, 785 °C and 739 °C, respectively. The estimated temperatures are higher than that onset of FS [13], consequently the flash sintering process is maintained. The flash effect at this moment is accompanied by the oxidation of graphite. In the last constant current control stage, the power dissipation keeps at 920 mW mm^{-3} for 10 min. The estimated temperature of the specimen is 1285 °C, determined by the power dissipation value (see Table 1). Of course, only Joule heating alone cannot explain the flash sintering phenomenon. The possible theory proposed that the applied field and the higher specimen temperature act synergistically can produce an avalanche of defects, such as Frenkel pairs, that greatly enhance the rate of mass transport [21].

The specimen electrical conductivity strongly depends upon the actual temperature during flash sintering. Fig. 4 presents the variations of conductivity (in a logarithmical scale) with the specimen temperature estimated by the above blackbody radiation model. There are two curves that represent different process, which are the voltage control stage and current control stage, respectively. The blank area in the middle is not listed, corresponding to the stage of graphite oxidation. From Fig. 4, it can be seen that the temperature-dependent conductivity thoroughly follow an Arrhenius relation in the voltage control stage ($R^2 = 0.998$). The calculated activation energy E is 0.30 eV, which is consistent with the value reported by Luo (~0.30 eV, ZnO specimen during flash sintering in Ar + 5 mol% H_2) [11]. The lower activation energy in the voltage control stage is in relation to the electronic conduction of

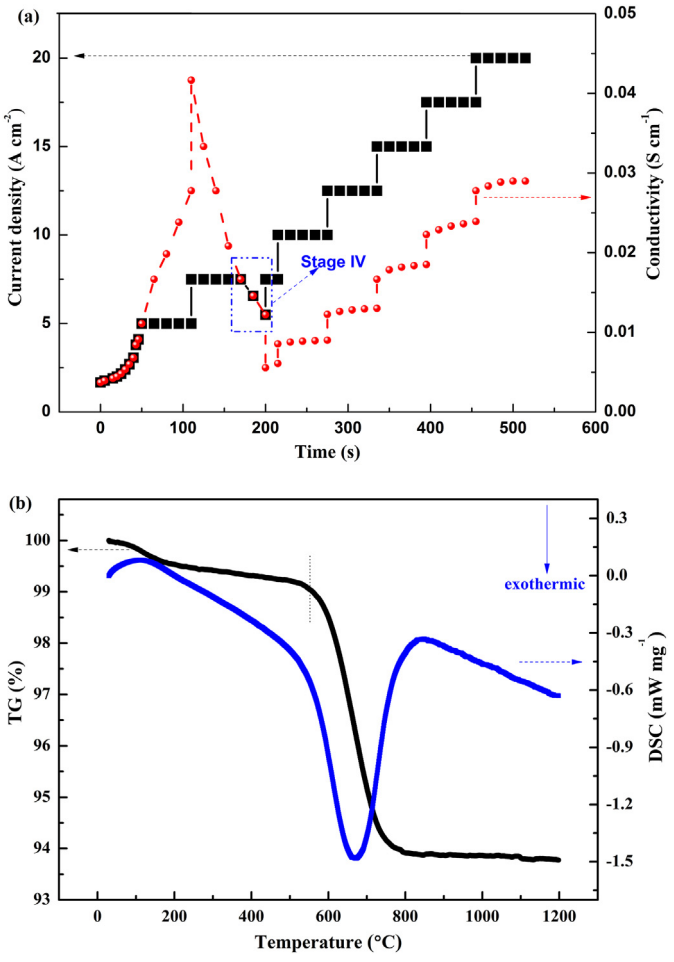

Fig. 2. The behaviours associated with the graphite assisted flash sintering (a) the variation curves of the current density and electrical conductivity with time and (b) TG and DSC curves of SDC-5 wt% graphite composite green compact in air.

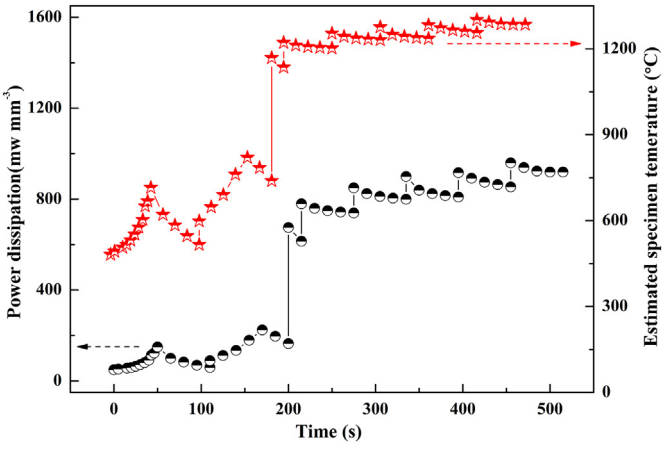

Fig. 3. Power dissipation and estimated specimen temperature curves of graphite assisted flash sintering.

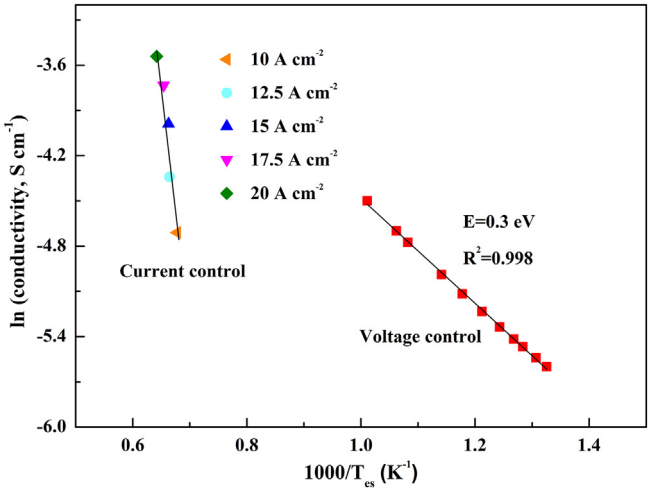

Fig. 4. Measured electrical conductivity vs. the estimated specimen temperature curves during graphite assisted flash sintering.

graphite. The activation energy increases rapidly to 2.93 eV when the graphite is completely oxidized (Note that the data under current control determined by the result of quasi-steady state in each regime), this is consistent with the conventional flash sintering. This may be explained by the mixed ionic and electronic conduction of SDC at high temperatures.

In summary, this study demonstrated the graphite assisted flash sintering technique can be realized preparation of dense SDC ceramics at room temperature. The current increases non-linearly to a set limit value in the voltage control stage under an initial electric field of 30 V cm^{-1}, the calculated activation energy is 0.30 eV in this stage. This is in relation to the electronic conduction of graphite. The electrical conductivity sharply increases to the peak value, and then decreases rapidly, which should be ascribed to the existence and oxidation of graphite. When graphite is completely oxidized, the estimated temperatures are higher than the onset of conventional flash sintering, consequently the flash sintering process is maintained. The sintered SDC at the current density of 20 A cm^{-2} for 10 min showed a dense and fine grained structure. The GAFS technique provides a novel approach to flash sintering of ceramics at room temperature.

Acknowledgment

This work is financially supported by the Innovation Funds for the Inner Mongolia University of Science and Technology (No. 2016QDL-B15), and supported by the National Natural Science Foundation of China (Grant No. 51762036 and No. 51464038).

References

[1] M. Cologna, B. Rashkova, R. Raj, J. Am. Ceram. Soc. 93 (2010) 3556–3559.
[2] M. Cologna, A.L.G. Prette, R. Raj, J. Am. Ceram. Soc. 94 (2011) 316–319.
[3] K. Sun, J. Zhang, T. Jiang, J. Qiao, W. Sun, D. Rooney, Z. Wang, Electrochim. Acta 196 (2016) 487–495.
[4] A.L.G. Prette, M. Cologna, V. Sglavo, R. Raj, J. Power Sources 196 (2011) 2061–2065.
[5] A. Gaur, V.M. Sglavo, J. Mater. Sci. 49 (2014) 6321–6332.
[6] S.K. Jha, R. Raj, J. Am. Ceram. Soc. 97 (2014) 527–534.
[7] Y.Y. Zhang, J.I. Jung, J. Luo, Acta Mater. 94 (2015) 87–100.
[8] K. Naik, S.K. Jha, R. Raj, Scr. Mater. 118 (2016) 1–4.
[9] D. Yadav, R. Raj, Scr. Mater. 134 (2017) 123–127.
[10] J.A. Downs, V.M. Sglavo, J. Am. Ceram. Soc. 96 (2013) 1342–1344.
[11] Y. Zhang, J. Luo, Scr. Mater. 106 (2015) 26–29.
[12] J. Nie, Y. Zhang, J.M. Chan, R. Huang, J. Luo, Scr. Mater. 142 (2018) 79–82.
[13] J. Li, L.L. Guan, W. Zhang, M. Luo, J.L. Song, X.W. Song, S.L. An, Ceram. Int. 44 (2018) 2470–2477.
[14] Z. Shen, M. Johnsson, Z. Zhao, M. Nygren, J. Am. Ceram. Soc. 85 (2010) 1921–1927.
[15] Y.Y. Zhang, J.Y. Nie, J.M. Chan, J. Luo, Acta Mater. 125 (2017) 465–475.
[16] H. Charalambous, S.K. Jha, K.H. Christian, R.T. Lay, T. Tsakalakos, J. Eur. Ceram. Soc. 38 (2018) 3689–3693.
[17] K. Ren, Q. Wang, Y. Lian, Y. Wang, J. Alloys Compd. 747 (2018) 1073–1077.
[18] P.D.S.J. Gustavo, J. Lebrun, H.A. Al-Qureshi, R. Janssen, R. Raj, J. Am. Ceram. Soc. 98 (2015) 3525–3528.
[19] R.I. Todd, E. Zapata-Solvas, R.S. Bonilla, T. Sneddon, P.R. Wilshaw, J. Eur. Ceram. Soc. 35 (2015) 1865–1877.
[20] X. Su, G. Bai, Y. Jia, Z. Wang, W. Wu, J. Eur. Ceram. Soc. 38 (2018) 3489–3497.
[21] R. Raj, J. Eur. Ceram. Soc. 32 (2012) 2293–2301.